

[dx.doi.org/10.17488/RMIB.42.2.7](https://dx.doi.org/10.17488/RMIB.42.2.7)

E-LOCATION ID: 1140

## Feature Extraction from Distributions of Phase Synchronization Values of EEG Recordings

J. A. Quirarte-Tejeda<sup>1</sup>, J. L. Flores<sup>1</sup>, R. Romo-Vázquez<sup>2</sup>

<sup>1</sup>Departamento de Electrónica, CUCEI, Universidad de Guadalajara

<sup>2</sup>Departamento de Ciencias Computacionales, CUCEI, Universidad de Guadalajara

### ABSTRACT

Epilepsy is the most common neurological pathology. Despite treatments available to patients, only 58% to 73% will be free of seizures. This uncertainty in treatment outcomes can lead to other psychiatric affectations in cases where treatment success may be in doubt. Seizure prediction models (SPMs) emerged as a measure to help determine when patients may be susceptible to an imminent crisis. These models are based on the continuous monitoring of patient's EEG signals and subsequent continuous analysis to identify features that differentiate ictal from interictal states. This is an ongoing field of research whose aim is to establish a robust set of features to feed the SPM and obtain a high degree of certainty regarding when the next seizure will occur. In this work we propose the analysis of phase differences of EEG as a method to extract features capable of discriminating ictal and preictal states in patients; specifically, the numeric distance between Q1 and Q3 of the distribution of phase differences. We compared this values to other phase synchronization methods and tested our hypothesis getting a  $p < 0.0009$  with our proposed method.

**KEYWORDS:** Epilepsy; Phase analysis; Synchronization; Phase differences

### Corresponding author

TO: Rebeca del Carmen Romo Vázquez

INSTITUTION: Universidad de Guadalajara

ADDRESS: Blvd. Gral. Marcelino García Barragán #1421,

Col. Olímpica, C. P. 44430, Guadalajara, Jalisco, México

E-MAIL: [rebeca.romo@academicos.udg.mx](mailto:rebeca.romo@academicos.udg.mx)

### Received:

2 December 2020

### Accepted:

11 March 2021

## INTRODUCTION

Epilepsy is the most common neurological disorder, affecting around 30 million people worldwide <sup>[1]</sup>. At a neurological level, epilepsy manifests itself as electrical discharges in neuron populations, that can produce muscular contractions and loss of consciousness <sup>[2] [3] [4] [5] [6]</sup>. These disorders affect the daily life of patients and impedes them from performing certain tasks at work, driving, and swimming when unsupervised; hence, the interest in researching new ways to diagnose and treat epilepsy.

Current treatments for epilepsy involve drugs that can reduce the incidence and/or intensity of seizures up to a 70% of patients. For the remaining 30%, who have drug-resistant epilepsy, other treatments are being tested. Of these, brain surgery has been the most successful <sup>[4]</sup>. Brain surgery, however, is not a viable treatment in all cases, and even when performed, only 58% to 73% of patients will be free of impairing seizures <sup>[7] [8]</sup>.

Despite the ratio of success of surgical procedures and drug treatments, patients who suffer impairing epileptic seizures are also prone to suffering other psychiatric affections, such as anxiety and depression <sup>[7] [8]</sup>, both caused by the uncertainty as to when the next seizure will occur. The unpredictable nature of epilepsy and the lack of understanding of how *epileptogenic* conditions emerge in the brain, have led to the development of several techniques for estimating the beginning or *onset* of an epileptic seizure <sup>[8]</sup>. The aim is to understand the conditions that lead to seizures and use this information in seizure prediction models in order to prevent the *onset* of epileptic crises in patients.

Most seizure prediction models (SPMs) are based on the analyses of recorded electroencephalographic signals (EEG), a common diagnostic procedure. SPMs derived from analyses of EEG signals are constrained to physiological and mathematical assumptions <sup>[9]</sup>: the former holds that changes in brain activity and its

associated electrical signals appear before seizures and can be acquired by EEG, while the mathematical assumption refers to a commonly implicit, but not well understood, statistical relationship between past and future observations of the EEG signals. These two assumptions lead to consider that is possible to predict seizures based on EEG recordings <sup>[9]</sup>.

In general, SPMs based on EEG signal processing, consist of three stages <sup>[10, 11]</sup>: preprocessing the EEG signals, extracting features from them, and classifying of brain electrical activity. One current challenge in this approach is to successfully discriminate the different epileptic seizure stages such as *interictal*, *pre-ictal*, *ictal* and *post-ictal* stages <sup>[9] [10] [11] [12] [13] [14]</sup>.

Depending on the method used in feature extraction, SPMs can be classified as: time-frequency methods, nonlinear measures, or statistical parameters of the signals <sup>[8] [10] [14]</sup>. Most of the time-frequency methods -e.g. as spectral power and connectivity- only function under certain limitations related to a limited temporal resolution. Additionally they assume linear interactions of the signals and disregard non-stationary properties <sup>[15]</sup>. Nonlinear methods are preferred since it is assumed that they preserve the nonlinear nature of EEG signals <sup>[10]</sup> which is closer to their real behavior <sup>[16]</sup>.

Phase synchronization analysis of EEG signals is now a promising approach for understanding brain dynamics because it has shown that some changes occur in the synchronization and connectivity of brain networks during seizures <sup>[17]</sup>. The premise is that different areas of the brain may come to be connected between each other during an epileptic seizure <sup>[6]</sup>; that is. two distinct brain regions with oscillatory electrical activity will show phase synchronization though they are not anatomically adjacent. This phenomenon is known as *functional connectivity*. It has been widely reported that *functional connectivity* can be affected by brain pathologies, such as epilepsy <sup>[21]</sup>.

In the past decade, synchronization indexes have been used in epilepsy analyses during *preictal/ictal* stages, Haitao *et al.* for example, showed that synchronization between distant areas of the brain increases in epileptic patients [18]. While Alaei *et al.* [19] proposed the mean phase coherence index as a feature to determine the preictal stage in patients, and Detti *et al.* [12] proposed an SPM whose features, obtained from synchronization measurements in ictal and preictal stages, was able to predict the *onset* of seizures with high accuracy. These features were obtained by analyzing phase synchronization between each pair of EEG channels and selecting the most appropriate pair by inspection.

In this work, we propose the instantaneous phase difference index (PDI) as an alternative approach for analyzing EEG signals to discriminate the *preictal/post ictal* and ictal stages. To this end we compared the performance of our index against *Phase Locking Value* (PLV), *Phase Lag Index* (PLI) and *Phase Linearity Measurements* (PLM) in two EEG databases and applied a Kruskal-Wallis test based on characteristics of their phase differences or synchronization value distributions in each epileptic stage.

## MATERIALS AND METHODS

### Databases

In this work we analyzed two databases. The first consists of EEG recordings and the second of intracranial EEG recordings (iEEG).

#### Database 1

These EEG signals were obtained from Zenodo “A dataset of neonatal EEG recordings with seizure annotations” [20]. This dataset contains 79 recordings of neonates acquired by a clinical team due to suspicions of seizure activity. The EEG recordings have an average recording time of 74 min, and were recorded with a NicOne EEG amplifier using a sample frequency of

256Hz, with 19 electrodes positioned according to the 10-20 International System with referential montage. Two additional channels were included in the recording, which contain ECG and respiratory signals from the patients. Three experts (identified as A, B and C) were asked to individually annotate seizures with a clear *onset* of abnormal electrical activity. Seizures were defined by a duration of over 10 seconds

Of the 79 initial recordings of patients in database 1, 29 were chosen for further analysis because they showed lateralized epileptic seizure annotations. However, based on the criterion that at least two of the experts had to agree on the starting times, only 20 seizure events were chosen.

A window containing 15 seconds before and 15 seconds after the starting time of the seizure was cropped from the original recording and preprocessed for further analysis.

#### Database 2

Database 2 consists of iEEG signals, obtained from the “American Epilepsy Society Seizure Prediction Challenge”. It contains a variable number of interictal/ictal test samples of one second iEEG recordings for each subject. For our work only the first 20 interictal samples and the first 20 ictal samples per subject were chosen for further analysis. The number of channels also varied from subject-to-subject, but all channels available from each subject were used in the subsequent analysis.

### Methods

Phase synchrony metrics has been proposed as a way to estimate the degrees of functional connectivity [2]. Most of the approaches proposed to analyze connectivity are based on the frequency domain and operate under certain assumptions such as: stationary signals and limited temporal resolution. These techniques also assume linear behavior and interactions between

signals [15]. But these considerations are not always consistent with the real behavior and properties of EEG signals.

We consider EEG to be the result of nonlinear dynamic processes in the brain, and seizure events as a non-stationary process [16] that may be evidenced by changes in phase synchrony indexes before and after the *onset*.

### Phase Locking Value (PLV)

In literature, several phase-based indexes have been proposed, one of which is the *Phase Locking Value* (PLV), proposed in [15]. PLV was the first synchronization index approach to determine the synchronization between two signals in terms of their phase,  $\varphi_1$  and  $\varphi_2$  as:

$$PLV = \frac{1}{N} \sum_1^N e^{j(\Delta\varphi)} \quad (1)$$

where  $\Delta\varphi$  is the phase difference between two signals whose synchronization is being estimated.

In this sense, PLV has a range of 0-1, where 0 corresponds to no synchrony and 1 represents total synchrony between signals. Lachaux *et al.* introduced the  $N$  term in order to test the synchrony of both signals against  $N$  trials, expecting a reduction of spontaneous synchronization.

### Phase Lag Index (PLI)

Another approach to determining the synchrony between two signals is the *Phase Lag Index*, (PLI), proposed in [22]. In this case, synchrony is analyzed in terms of phase difference,  $\Delta\varphi$ , as

$$PLI = |\langle \text{sign}[\Delta\varphi] \rangle| \quad (2)$$

where  $\text{sign}[]$  is the sign function and  $\langle \cdot \rangle$  is the mean operator. PLI returns an index of synchronization in a range of 0-1. A PLI index equal to 1, means that the

phase difference between two signals modulus  $\pi$  is equal to zero, i. e. both signals contain information from the same brain source, and this value does not represent true synchronization.

### Phase Linearity Measurement (PLM)

A third method is *Phase Linearity Measurement* (PLM), proposed by Baselice *et al.* [23]. PLM analyzes phase differences as a function of time in narrow frequency bands, from  $-B$  to  $B$ , that can be determined as

$$PLM = \frac{\int_{-B}^B \left| \int_0^T e^{j(\Delta\varphi(t))} e^{-j2\pi ft} dt \right|^2 df}{\int_{-\infty}^{\infty} \left| \int_0^T e^{j(\Delta\varphi(t))} e^{-j2\pi ft} dt \right|^2 df} \quad (3)$$

This approach introduces a first order model phase differences that is dependent on the instantaneous frequency of the signal, instead of a constant one, as in the PLV and PLM indexes.

### Phase Difference Index (PDI)

From Equations (1), (2), and (3) we can observe that the PLV, PLI and PLM indexes are surjective functions over the  $\Delta\varphi$  set. However, the use of surjective functions does not preserve the full relationships between the elements of the set applied to, resulting in information loss.

Phase difference  $\Delta\varphi$  is a discrete variable, with values in a range of  $\pi$  to  $-\pi$ , whereas the PLV, PLI and PLM functions all have a range of 0-1. This limited range also results in information loss that can be demonstrated by calculating the probability of any outcome  $\delta_1$  for the  $\Delta\varphi$  and the probability of the outcome  $x_1$  for any variable  $X$  in a range from 0-1; thus  $P(\delta_1) < P(x_1)$ . Through Shannon's entropy definition [24], we can show that:

$$P(\delta_1) < P(x_1) \quad (4)$$

so variable  $\Delta\varphi$  has greater entropy than  $X$ .

This difference in entropy from  $\Delta_\varphi$  to  $X$  led us to consider that this reduced range of the codomain of the PLV, PLI and PLM functions might be hiding part of the chaotic behavior of the EEG recordings. Hence, to avoid surjective functions we propose the *Phase Difference Index (PDI)*, as an adequate means of analyzing the phase synchronization of EEG signals:

$$PDI = \frac{\varphi_1 - \varphi_2}{k} \quad (5)$$

where  $\varphi_1$  and  $\varphi_2$  are two phase vectors of  $k$  length.

The use of phase differences to analyze EEG scalp signals could lead to the detection of spurious phenomena caused mainly by volume conduction [22] [23]. In order to test whether this phenomenon affects the ability of phase differences to discriminate preictal/ ictal signals, we calculated the phase differences: PLV, PLI and PLM indexes for database 2, which consists of intracranial EEG recordings (iEEG), where volume conduction effects are not present.

Figure 1 depicts a block diagram of proposed algorithms, where we can see the different stages in the processing of EEG signals.

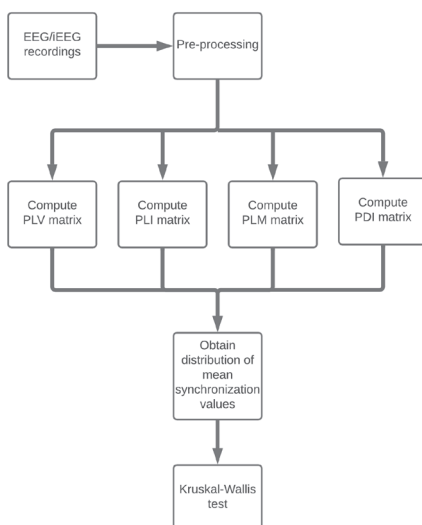


FIGURE 1. Data processing scheme.

## Database pre-processing

In both databases a band-pass filter was applied with a bandwidth of 4Hz-6Hz (i. e. *theta* range). Specifically, we applied a zero phase FIR filter of 20th order, due zero padding and floating-point values of the FIR filter which results in non-zero DC gain. In this way, the DC component in the filtered signals was removed. Additionally, since the EEG signals in database 2 had a sampling frequency of 500Hz to 5000Hz, all recordings were downsampled to 500Hz.

## Instantaneous phase calculation

As our aim was to obtain phase values from each sample of the signal, we considered each recording as an array of  $N$  signals obtained from electrodes placed on the brain according to the 10-20 International System.

In order to retrieve the instantaneous phase for each EEG signals ( $s(k)_n$  for  $n = 1, 2, \dots, N$ ), we constructed an analytic signal as

$$x_n(k) = s_n(k) + j\hat{s}_n(k) \quad (6)$$

where  $\hat{s}_n(k)$  is the *Hilbert Transform* of  $s_n(k)$ . From the Eq. (6) we can retrieve the phase value  $\varphi(k)$  for each EEG sequence as

$$\varphi_n(k) = \arctan \frac{\hat{s}_n(k)}{s_n(k)} \quad (7)$$

For each phase vector  $\varphi_n(k)$  obtained from the EEG signal, we can compute the degree of phase synchronization between these EEG signals. PLV, PLI, PLM and PDI were calculated using a window of half-second or 128 samples, sliding one sample at a time. The size of the window was selected as a trade-off between the capacity to observe brain network reorganization on the sub-second time scale, as reported in [25] and to detect synchronization on the second-scale, as described in [15] [16] [17] [18] [19] [20] [21] [22].

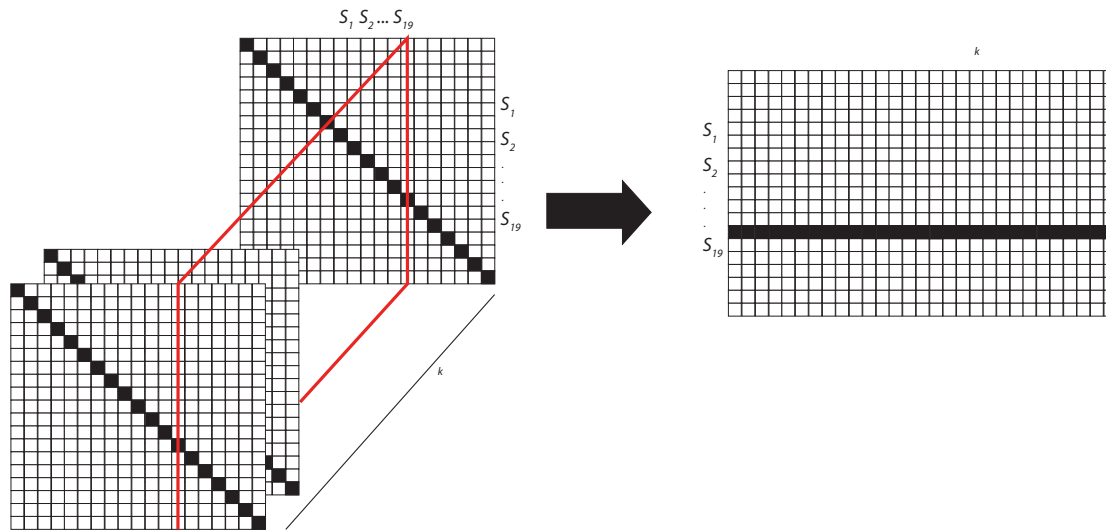


**FIGURE 2. Synchronization/phase difference matrix structure. The red slice can be extracted to visualize changes in synchronization/phase differences over time.**

### Synchronization and phase difference matrices

For database 1, the synchronization values for PLV, PLI, PLM and PDI were obtained from  $s(k)_n$  for  $k = 0$  and stored in a  $19 \times 19$  matrix. Each cell corresponds to a possible combination of the  $n$  available channels. Since Eqs. (1), (2) and (3) do not preserve the sign of the phase difference, therefore PLV, PLI and PLM are commutative between a pair of signals. As a result, the synchronization matrix will be symmetrical, with the main diagonal representing the synchronization of a given signal with itself. The diagonal of the PDI matrix will have a value of zero since it corresponds to the difference between signals from the same source. The same procedure was applied to the next sample of each sequence  $s(k)_n$  for  $k = 1$  and the resulting new  $19 \times 19$  matrix was stacked behind the previous one until the sliding window reached the last sample  $s(k)_n$  for  $k = 7554$ . This resulted in a 3D matrix with  $19 \times 19 \times 7554$  elements for each synchronization index PLV, PLI, PLM and PDI for each seizure event selected from database 1.

The matrices obtained can be used to show how synchronization or phase differences change over time when sliced them along the  $k$  dimension, see Figure 2.

The column index from which the slice is extracted defines the reference signal to determine the temporal evolution of the synchronization or phase difference, respectively.

Since each matrix contains information pre- and post- seizure onset, the onset information will be in the center, along the  $k$  length, as Figure 2 shows. We can split each matrix in two along the  $k$  length to separate the information from preictal to ictal stages (see Figure 3).

For the database 2 recordings, the data processed by means of PLV, PLI, PLM and PDI were stored in matrices with the same structure as before. The only difference was in their dimensions, since each of the subjects' recordings had distinct number of available channels.

### Distributions of synchrony/phase difference values

Each matrix has dimension  $N \times N \times k$ , to analyze how the synchrony indexes and phase difference change as a function of time during the different epilepsy stages, we took a  $N \times N$  matrix along the  $k$  dimension and gen-

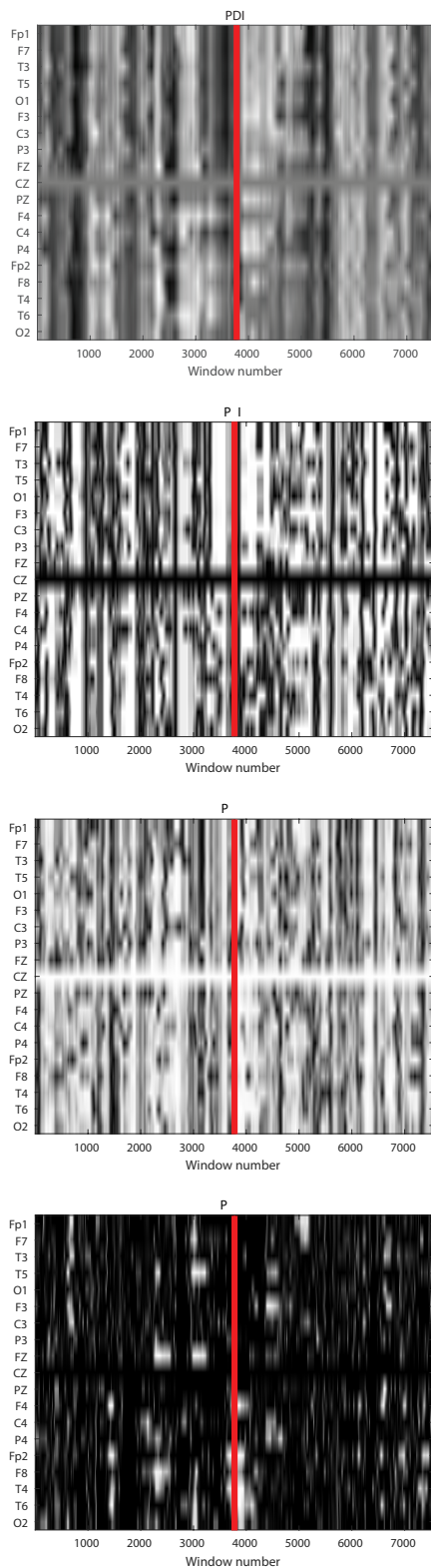


**FIGURE 3.** Grayscale map of slices along the Cz channel of the PDI, PLV, PLI and PLM matrices. A darker shade indicates a lower synchronization level. The line indicates the onset of the seizure.

erated a vector of length  $N$  with the average synchrony or phase difference values of each channel. The first element of the vector corresponds to the average value of the channel 1 in the first  $N \times N$  matrix. We then proceeded to the following  $N \times N$  matrices until reaching the last one. At the end we obtained  $k$  number of vectors of  $N$  length. Finally, we plotted the histogram of values of all the resulting vectors and then repeated the process with all the matrices.

Given that the *ictal* matrices were separated from the *preictal/interictal* ones, we displayed the histograms from between the *ictal* and *preictal* events. For both database 1 and database 2 recordings. We compared the *ictal* histograms to the corresponding *interictal* histograms.

Finally, we averaged the histograms per subject and analyzed how the distribution varied from the *ictal* stages to the *interictal/preictal* stages. We observed that the histograms corresponding to the *interictal/preictal* stages tended to have greater dispersion than the *ictal* ones, these changes in dispersion led us to choose the numeric distance between the first,  $Q1$  and the third quartiles,  $Q3$ , as a discriminator for the *ictal* and *interictal/preictal* stages of an epileptic event. A Kruskal-Wallis test was performed to probe our hypothesis.

## RESULTS AND DISCUSSION

Figures 4 and 5 show box plots of the mean phase differences and mean values of the PLV, PLI and PLM histograms for the *ictal* and *preictal/interictal* states, retrieved from an EEG recordings in databases 1 and 2. We observed that changes in the distribution of the mean values of the histograms between the *ictal* and *interictal* stages of the seizure were more evident when the recordings were analyzed by PDI, whereas the distribution of the mean values of the histograms for PLV, PLI and PLM indexes showed only small changes between seizure stages.

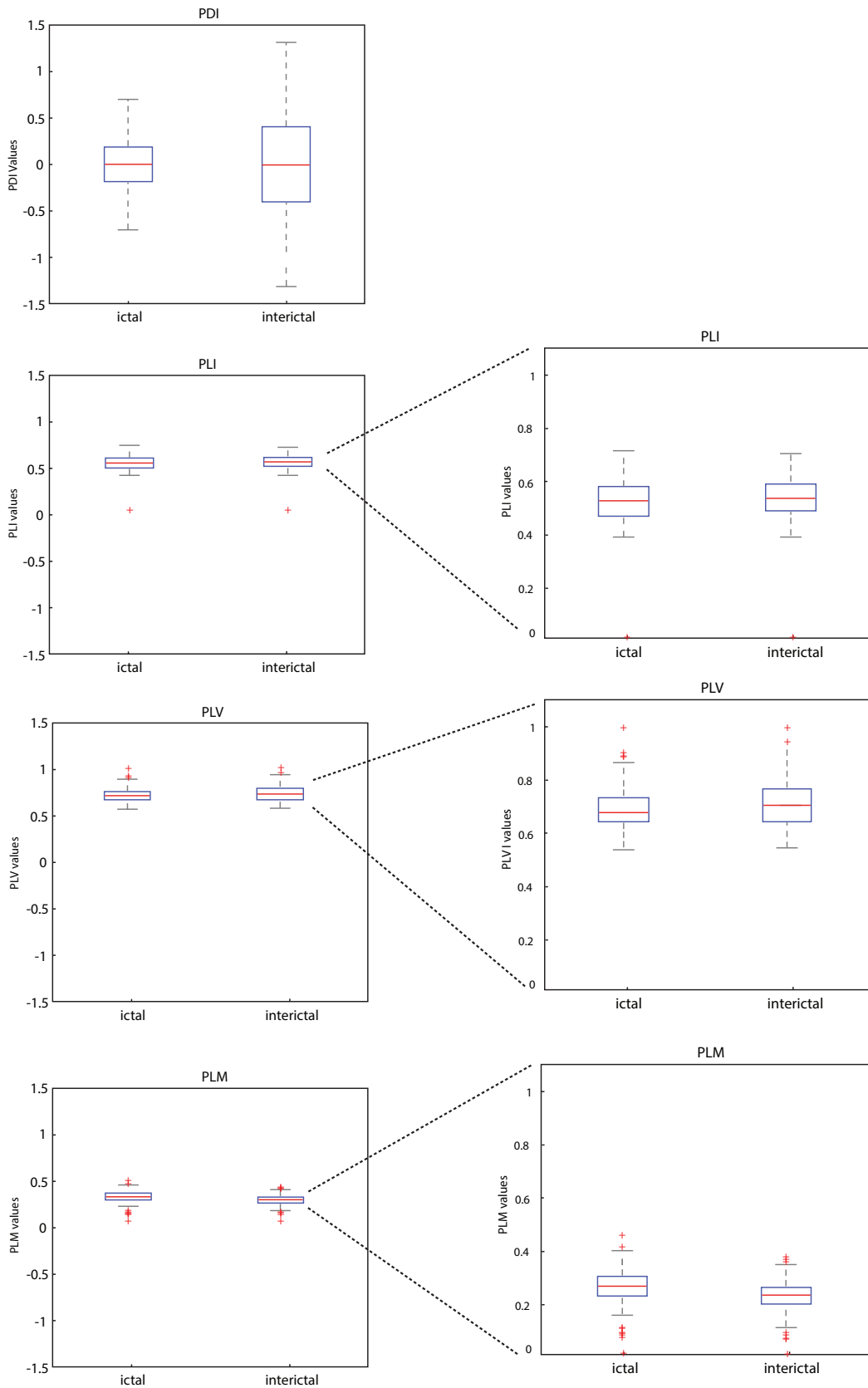


**FIGURE 4.** Grayscale map of slices along the Cz channel of the PDI, PLV, PLI and PLM matrices. A darker shade indicates a lower synchronization level. The line indicates the *onset* of the seizure.

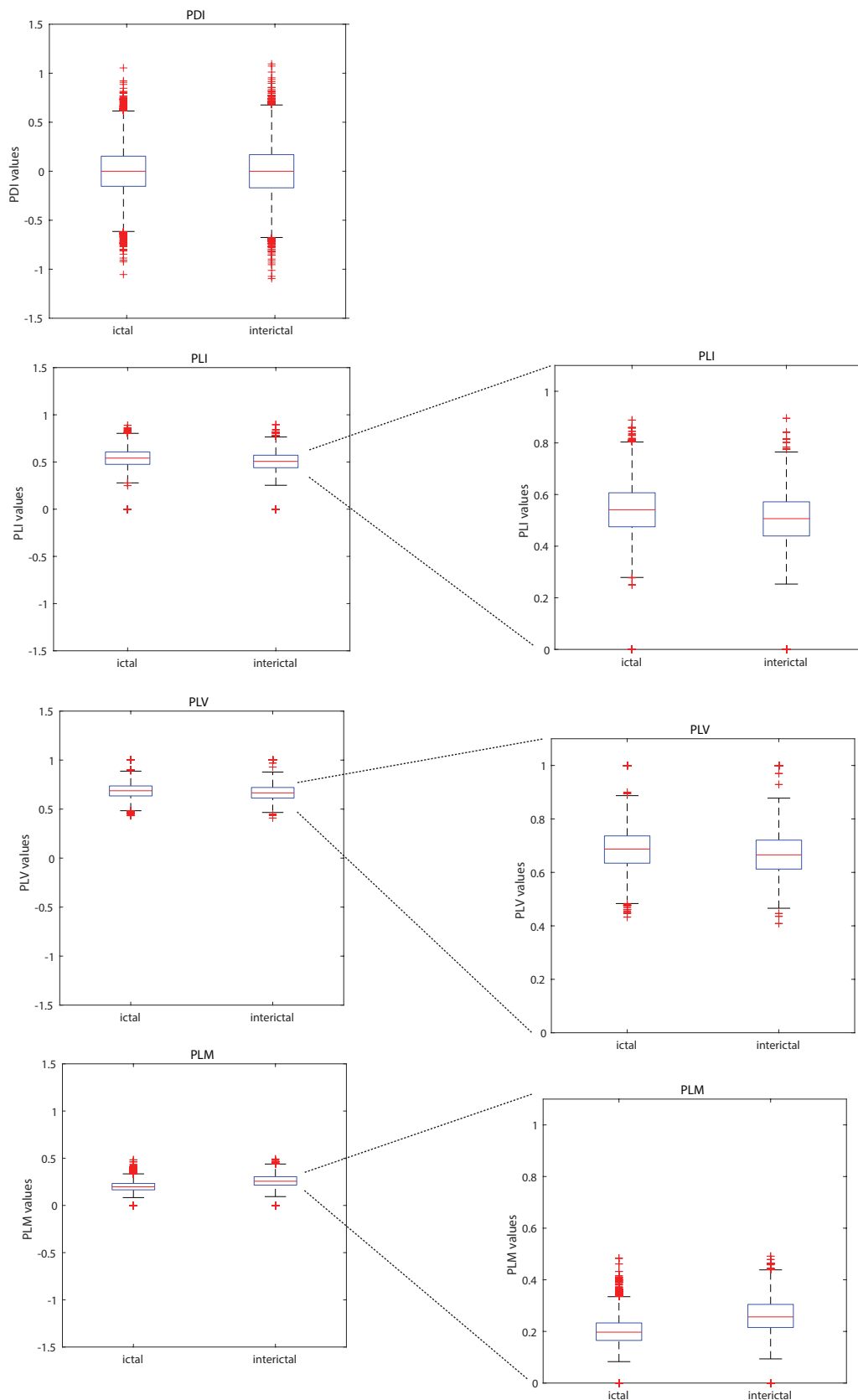


**FIGURE 5.** Distributions of the mean PDI, PLV, PLI and PLM values for a crisis selected from database 2. The left column shows the distributions at the same scale; the right column shows the zoomed-in distributions of PLI, PLV and PLM.

Tables 1 and 2 summarize the results of the Kruskal-Wallis test applied to the indexes computed from the recordings in databases 1 and 2, respectively. In both cases, the PDI performed better than PLV, PLI and PLM

indexes under our testing conditions. Tables 3 and 4 summarize the Q1, Q2 and Q3 values of the distributions of the mean histograms for the PLV, PLI, PLM and PDI indexes for the *ictal* and *preictal* stages.

**TABLE 1. Kruskal-Wallis test results for each index of the database 1 EEG recordings**

Index	p-value
PLV	0.2235
PLI	0.3169
PLM	0.6263
PDI	0.0008

**TABLE 2. Kruskal-Wallis test results for each index of the database 2 EEG recordings**

Index	p-value
PLV	0.0615
PLI	0.4132
PLM	0.0086
PDI	0.0013

A similar performance was observed for the recordings from database 2. As the PLI and PLM indexes were developed to reduce spurious synchronization values caused by volume conduction, but PLV and PDI are susceptible to this, database 2 provided a scenario with no advantage to any index. In this case it was evident that under no volume conduction effects, PDI also performed better than the other three indexes, suggesting that PDI preserves information that is useful for discriminating the stages of epileptic seizures. This results are consistent with the results reported

previously in [26] where the authors found no significant changes in the PLI mean value between the *preictal* and *ictal* stages.

Overall, our proposed index, PDI, showed a better performance in feature extraction based on the distribution analysis of phase synchronization values than other indexes developed previously. Implementing our proposed index in the processing stages of SPMs offers a feature that was not previously revealed by existing phase synchronization indexes.

**TABLE 3. Q1, Q2 and Q3 values for the mean histograms of the for PLV, PLI, PLM and PDI values computed for Database 1.**

Index	Q1 <i>preictal</i>	Q2 <i>preictal</i>	Q3 <i>preictal</i>	Q1 <i>ictal</i>	Q2 <i>ictal</i>	Q3 <i>ictal</i>
PLV	0.091618	0.11099	0.12004	0.083648	0.098677	0.11634
PLI	0.08535	0.10345	0.12568	0.080434	0.094336	0.10965
PLM	0.061742	0.077533	0.10111	0.068173	0.083978	0.11099
PDI	0.40871	0.74746	0.94231	0.26251	0.36316	0.52263

**TABLE 4. Q1, Q2 and Q3 values for the mean histograms of the for PLV, PLI, PLM and PDI values computed for Database 2.**

Index	Q1 <i>preictal</i>	Q2 <i>preictal</i>	Q3 <i>preictal</i>	Q1 <i>ictal</i>	Q2 <i>ictal</i>	Q3 <i>ictal</i>
PLV	0.2369	0.31682	0.37125	0.15321	0.28253	0.37855
PLI	0.58824	0.66667	0.70588	0.58824	0.64706	0.70588
PLM	0.32242	0.38348	0.45536	0.2595	0.35476	0.4189
PDI	2.3803	2.8566	3.2211	2.0286	2.5791	3.0129

## CONCLUSIONS

We found that changes in synchrony occur during the onset of a seizure and could be detected by phase analysis of EEG signals. The changes in the distribution of synchronization values before and after onset identified with the proposed PDI index suggest non-stationary behavior of EEG signals as reported in [16].

The phase difference index (PDI) can be used as a feature to discriminate *ictal* and *preictal/interictal* stages with good accuracy. It offers the advantage of using a simple algorithm that results in less intensive computational tasks and has potential applications in the development of SPMs which can operate in almost real time, and be implemented in portable devices. Further development of feature extraction using PDI can be extended using of broadband phase estimation methods.

The main limitations of the PDI approach is the need for a narrow frequency band in order to obtain interpretable results, this means that a priori knowledge of the spectral distribution of energy of the seizure events is required. We recognize that this approach neglects interactions that may occur between differ-

ent frequency bands. Although approaches to calculating broadband synchronization between signals have been developed [26] [27], they still have the limitation of being surjective functions that, as the presented work shows, can obfuscate information contained in the EEG recording.

## AUTHOR CONTRIBUTIONS

J.A.Q.T., J.L.F and R.R.V. conceived and designed the analysis, validation and writing-review and editing; J.A.Q.T. and R.R.V. performed the analysis; J.A.Q.T. investigation and writing original draft preparation; J.F.L. and R.R.V. supervision. All authors have read and agreed to the published version of the manuscript.

## ACKNOWLEDGEMENTS

The authors thank Francisco J. Alvarado Rodríguez for his valuable assistance and suggestions during this work.

## FUNDING

J.A. Quirarte-Tejeda was supported by CONACYT scholarship No. 716724. This research received no additional external funding.

## REFERENCES

- [1] Acharya UR, Sree SV, Swapna G, et al. Automated EEG analysis of epilepsy: A review. *Knowl-Based Syst* [Internet]. 2013;45:147-65. Available from: <https://doi.org/10.1016/j.knosys.2013.02.014>
- [2] Bruña R, Maestú F, Pereda E. Phase locking value revisited: teaching new tricks to an old dog. *J Neural Eng* [Internet]. 2018;15(5):056011. Available from: <https://doi.org/10.1088/1741-2552/aacfe4>
- [3] Fisher RS, Acevedo C, Arzimanoglou A, et al. ILAE Official Report: A practical clinical definition of epilepsy. *Epilepsia* [Internet]. 2014; 55(4):475-82. Available from: <https://doi.org/10.1111/epi.12550>
- [4] Nair DR. Management of Drug-Resistant Epilepsy. *Continuum (Minneapolis, Minn)* [Internet]. 2016;22(1):157-72. Available from: <https://doi.org/10.1212/con.0000000000000297>
- [5] Sejnowski TJ, Churchland PS, Movshon JA. Putting big data to good use in neuroscience. *Nat Neurosci* [Internet]. 2014;17:1440-1. Available from: <https://doi.org/10.1038/nn.3839>
- [6] van Mierlo P, Papadopoulou M, Carrette E, et al. Functional brain connectivity from EEG in epilepsy: Seizure prediction and epileptogenic focus localization. *Prog Neurobiol* [Internet]. 2014;121:19-35. Available from: <https://doi.org/10.1016/j.pneurobio.2014.06.004>
- [7] Camfield P, Camfield C. Idiopathic generalized epilepsy with generalized tonic-clonic seizures (IGE-GTC): a population-based cohort with >20 year follow up for medical and social outcome. *Epilepsy Behav* [Internet]. 2010;18(1-2):61-3. Available from: <https://doi.org/10.1016/j.yebeh.2010.02.014>
- [8] Ramgopal S, Thome-Souza S, Jackson M, et al. Seizure detection, seizure prediction, and closed-loop warning systems in epilepsy. *Epilepsy Behav* [Internet]. 2014;37:291-307. Available from: <https://doi.org/10.1016/j.yebeh.2014.06.023>
- [9] Chen H-H, Cherkassky V. Performance metrics for online seizure prediction. *Neural Netw* [Internet]. 2020;128:22-32. Available from: <https://doi.org/10.1016/j.neunet.2020.04.022>
- [10] Acharya UR, Hagiwara Y, Adeli H. Automated seizure prediction. *Epilepsy Behav* [Internet]. 2018;88:251-61. Available from: <https://doi.org/10.1016/j.yebeh.2018.09.030>
- [11] Kuhlmann L, Lehnertz K, Richardson MP, et al. Seizure prediction –ready for a new era. *Nat Rev Neurol* [Internet]. 2018;14(10):618-30. Available from: <https://doi.org/10.1038/s41582-018-0055-2>
- [12] Detti P, Vatti G, Zabalo Manrique de Lara G. EEG Synchronization Analysis for Seizure Prediction: A Study on Data of Noninvasive Recordings. *Processes* [Internet]. 2020;8(7):846. Available from: <https://doi.org/10.3390/pr8070846>
- [13] Espinoza-Valdez A, González-Garrido A, Luna B, et al. Epileptic brain reorganization dynamics on the basis of the probability of connections. *NeuroReport* [Internet]. 2015;27(1):1-5. Available from: <https://doi.org/10.1097/WNR.0000000000000472>
- [14] Mormann F, Andrzejak RG, Elger CE, Lehnertz K. Seizure prediction: the long and winding road. *Brain* [Internet]. 2007;130(2):314-33. Available from: <https://doi.org/10.1093/brain/awl241>
- [15] Lachaux J-P, Rodriguez E, Martinerie J, Varela FJ. Measuring phase synchrony in brain signals. *Hum Brain Mapp* [Internet]. 1999;8(4):194-208. Available from: [https://doi.org/10.1002/\(SICI\)1097-0193\(1999\)8:4<194::AID-HBM4>3.0.CO;2-C](https://doi.org/10.1002/(SICI)1097-0193(1999)8:4<194::AID-HBM4>3.0.CO;2-C)
- [16] Klonowski W. Everything you wanted to ask about EEG but were afraid to get the right answer. *Nonlinear Biomed Phys* [Internet]. 2009;3(1):2. Available from: <https://doi.org/10.1186/1753-4631-3-2>
- [17] Fan M, Chou C-A. Detecting Abnormal Pattern of Epileptic Seizures via Temporal Synchronization of EEG Signals. *IEEE Trans Biomed Eng* [Internet]. 2019;66(3):601-8. Available from: <https://doi.org/10.1109/TBME.2018.2850959>
- [18] Yu H, Cai L, Wu X, et al. Investigation of phase synchronization of interictal EEG in right temporal lobe epilepsy. *Physica A* [Internet]. 2018;492:931-40. Available from: <https://doi.org/10.1016/j.physa.2017.11.023>
- [19] Alaei HS, Khalilzadeh MA, Gorji A. Online Epileptic Seizure Prediction Using Phase Synchronization and Two Time Characteristics: SOP and SPH. *Int Clin Neurosci J* [Internet]. 2019;7(1):16-25. Available from: <https://doi.org/10.15171/icnj.2020.03>
- [20] Stevenson N, Tapani K, Lauronen L, Vanhatalo S. A dataset of neonatal EEG recordings with seizure annotations. *Sci Data* [Internet]. 2019;6:190039. Available from: <https://doi.org/10.1038/sdata.2019.39>
- [21] Alducin Castillo J, Yanez Suárez O, Brust Carmona H. Electroencephalographic analysis of the functional connectivity in habituation by graphics theory. *RMIB* [Internet]. 2016;37(3):181-200. Available from: <https://doi.org/10.17488/RMIB.37.3.3>
- [22] Stam CJ, Nolte G, Daffertshofer A. Phase lag index: assessment of functional connectivity from multi channel EEG and MEG with diminished bias from common sources. *Hum Brain Mapp* [Internet]. 2007;28(11):1178-93. Available from: <https://doi.org/10.1002/hbm.20346>
- [23] Baseliçe F, Sorriso A, Rucco R, Sorrentino P. Phase Linearity Measurement: A Novel Index for Brain Functional Connectivity. *IEEE Trans Med Imag* [Internet]. 2019;38(4):873-82. Available from: <https://doi.org/10.1109/TMI.2018.2873423>
- [24] Shannon CE. 1 Shannon's Measure of Information. In: Aczél J, Daróczy Z (eds). *Mathematics in Science and Engineering* [Internet]. New York: Academic Press; Elsevier; 1975. 26-49p. Available from: [https://doi.org/10.1016/S0076-5392\(08\)62730-7](https://doi.org/10.1016/S0076-5392(08)62730-7)
- [25] Michel CM, Koenig T. EEG microstates as a tool for studying the temporal dynamics of whole-brain neuronal networks: A review. *NeuroImage* [Internet]. 2018;180:577-93. Available from: <https://doi.org/10.1016/j.neuroimage.2017.11.062>
- [26] Wang L, Long X, Aarts R, et al. A broadband method of quantifying phase synchronization for discriminating seizure EEG signals. *Biomed Signal Process Control* [Internet]. 2018;52:371-83. Available from: <https://doi.org/10.1016/j.bspc.2018.10.019>
- [27] Sorrentino P, Ambrosanio M, Rucco R, Baseliçe F. An extension of Phase Linearity Measurement for revealing cross frequency coupling among brain areas. *J Neuroeng Rehabil* [Internet]. 2019;16(1):135. Available from: <https://doi.org/10.1186/s12984-019-0615-8>